White dwarfs in the CFHTLS Deep fields

F. Limboz, Y. Karatas, M. Kilic, C. Benoist, S. Alis

Mon. Not. R. Astron. Soc. **383,** 957–961 (2008) doi:10.1111/j.1365-2966.2007.12636.x

White dwarfs in the CFHTLS Deep fields

F. Limboz,[1⋆] Y. Karataş,[1] M. Kilic,[2] C. Benoist[3] and S. Aliş[1]

[1]*Istanbul University, Science Faculty, Department of Astronomy and Space Sciences, 34119 Universite-Istanbul, Turkey*
[2]*Department of Astronomy, Ohio State University, Columbus, OH 43210, USA*
[3]*Observatoire de la Côte d'Azur, Laboratoire Cassiopée BP 4229, 06304 Nice Cedex 4, France*

Accepted 2007 October 24. Received 2007 October 10; in original form 2007 August 29

ABSTRACT

We present an initial assessment of white dwarfs in the third data release of the Canada–France–Hawaii Telescope Legacy Survey (CFHTLS) Deep fields. Following the morphological classification of point sources, we have selected the white dwarf candidates through colour cuts. A detailed comparison between the observed colours of the selected point sources with the expected colours of white dwarfs and quasars reveal 28 white dwarf candidates with $T_{\rm eff} \geqslant$ 5500 K. Eight of these candidates are spectroscopically confirmed to be white dwarfs, which demonstrates that our selection process is robust. Even though the *i*-band limiting magnitude of the Deep fields is $i \sim 26$ mag, we find that the star–galaxy separation is not reliable for $i > 21$. Using spectroscopic data from the VLT–VIRMOS Deep Survey, we quantify the contamination of our stellar sample by quasars and galaxies. Our catalogue of white dwarfs is incomplete, and further studies of the population of white dwarfs in the CFHTLS require accurate proper-motion measurements.

Key words: techniques: photometric – stars: evolution – white dwarfs.

1 INTRODUCTION

White dwarf stars are the remnants of the earliest and all subsequent generations of star formation and they are tracers of the age and evolution of the Galaxy. The white dwarf luminosity function of the Galactic disc has traditionally been used as a tool to estimate the star formation history and age of this population (Liebert 1979; Winget et al. 1987; Liebert, Dahn & Monet 1988). An investigation of the white dwarf luminosity function that is focused on disentangling theoretical uncertainties in the white dwarf cooling process would greatly benefit from a large sample of white dwarfs.

The Sloan Digital Sky Survey (SDSS) has greatly increased the number of spectroscopically confirmed white dwarf stars including hot (Eisenstein et al. 2006), cool (Kilic et al. 2006) and ultracool white dwarfs (Gates et al. 2004). Harris et al. (2006) created a new luminosity function using the proper-motion-selected sample of 6000 white dwarfs from the SDSS Data Release 3 (Munn et al. 2004). However, their sample had only 32 high-velocity white dwarfs that are likely to be members of the halo.

The Canada–France–Hawaii Telescope Legacy Survey (CFHTLS) Deep fields is a valuable new source to reveal faint white dwarf candidates in the Galactic disc and halo. Schultheis et al. (2006) studied the stellar population of the Deep survey using the first data release of the D1, D2 and D3 fields. The third data release of the Deep survey now provides deep *ugriz* photometry ($i \leqslant 26$ mag) for four fields, D1, D2, D3 and D4 covering a total area of 3.6 deg^2.

In this paper, we present a detailed analysis of the white dwarfs in the CFHTLS Deep fields. We use morphological classification to identify point sources and select white dwarf candidates out of these sources on the basis of their optical photometry. The organization of the paper is as follows. Section 2 describes CFHTLS fields and observations. Star–galaxy separation is discussed in Section 3, whereas our selection criteria for white dwarf candidates are discussed in Section 4. Our final catalogue of white dwarf candidates and results from this analysis are discussed in Section 5.

2 THE DATA

CFHTLS is a major observing programme that started in 2003 May and still continuing at the CFHT on Mauna Kea. The CFHTLS Deep survey is a subprogramme in this survey which has four Deep fields to monitor over five year duration of the project. A total of 202 nights are allocated to the Deep survey so far. At the end of the project, a total of $33^{\rm h}$, $33^{\rm h}$, $66^{\rm h}$, $132^{\rm h}$, $66^{\rm h}$ integration times are expected for the *u*, *g*, *r*, *i* and *z* bands in each field, respectively. All of the images were taken using the wide-field prime focus MegaPrime equipped with MEGACAM, a mosaic camera consisting 36 CCDs with 2048 $\times$ 4612 pixels. With its small pixel scale of 0.185 arcsec and the large number of nights dedicated to the survey, the CFHTLS goes deeper and has a better image quality than the SDSS, but on a much smaller area of the sky.

⋆E-mail: limboz@istanbul.edu.tr

Table 1. Summary of CFHTLS Deep fields for the T0003 release (Gavazzi & Soucail 2007).

	D1	D2	D3	D4
α_{2000}	$02^h\ 25^m\ 59^s$	$10^h\ 00^m\ 28^s$	$14^h\ 19^m\ 27^s$	$22^h\ 15^m\ 31^s$
δ_{2000}	$-04^o\ 29'\ 40''$	$+02^\circ\ 12'\ 30''$	$+52^\circ\ 40'\ 56''$	$-17^\circ\ 43'\ 56''$
l	172.°0	236.°7	96.°3	39.°2
b	−58.°0	+42°	+59.°7	−52.°8
u (mag)	26.5	26.1	25.9	26.5
g (mag)	26.4	26.2	26.6	26.3
r (mag)	25.0	26.0	26.4	26.4
i (mag)	25.9	25.7	26.2	26.0
z (mag)	25.0	24.9	25.1	25.0
Seeing (arcsec) (i)	0.91	0.95	0.91	0.87
Area (deg^2)	0.93	0.89	0.92	0.86

We use the object catalogues for the CFHTLS D1, D2, D3 and D4 fields that were released as part of the TERAPIX T0003 public release. Catalogues were produced by TERAPIX using SEXTRACTOR (Bertin & Arnouts 1996) dual image mode with a χ^2 image constructed from g, r, i images. Detailed description of this technique can be found in Szalay et al. (2003). Bad regions were masked out by visual inspection of the images. The coordinates (50 per cent completeness) limiting AB magnitudes, average seeing values, and sky coverage for these fields are listed in Table 1.

3 STAR-GALAXY CLASSIFICATION

Without proper-motion measurements, we rely on morphological classification of the point sources by SEXTRACTOR. We use the half-light radius (hereafter, HLR) measurements from the i-band images to identify stars. Schultheis et al. (2006) used the same method to study the stellar sample of the D1, D2 and D3 fields from the first data release of the CFHTLS Deep survey. HLR parameter measures the radius which encloses 50 per cent of the flux.

Fig. 1 presents i-band magnitude versus HLR for the objects in the D1 field. We note that the objects with $i < 17.00$ are saturated, and therefore have unreliable HLR measurements. It is clear from this figure that the point-like sources have HLR ∼2.4 pixel, and they are distinguishable from galaxies down to $i \sim 21$–22. In order to derive a robust selection mechanism for point sources, we use the optical spectroscopic data from the VIRMOS–VLT Deep Survey (VVDS; Le Fevre et al. 2005). The VVDS provides spectroscopy over the wavelength range 5500–9200 Å, and it overlaps with a small part of the D1 field. We select the stars and galaxies with 100 per cent confidence redshift measurements from the VVDS and cross-identify them with the sources in the D1 field using a search radius of 1 arcsec and constraining the i magnitudes from the two surveys to be within 1 mag of each other. We identify 361 stars and 1610 galaxies that are common to both VVDS and CFHTLS Deep survey. The mean difference between the positions from the two survey is 0.33 ± 0.16 arcsec^2 for stars and 0.33 ± 0.14 arcsec^2 for galaxies, whereas the mean difference in the i-band magnitudes is 0.23 ± 0.14 mag for stars and 0.11 ± 0.14 mag for galaxies. These spectroscopically confirmed stars and galaxies are shown as red circles and blue triangles in Fig. 1, respectively.

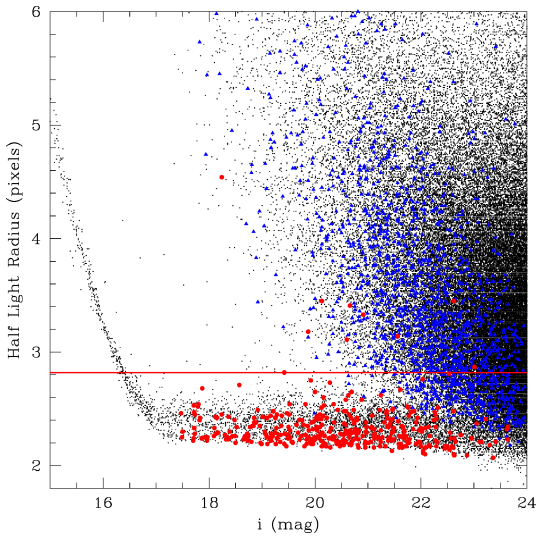

Figure 1. i-band magnitude versus HLR for the D1 field. The VVDS provides optical spectroscopy for a small section of the D1 field. Spectroscopically confirmed stars and galaxies from the VVDS are shown as red circles and blue triangles, respectively. Note that objects with $i < 17.00$ are saturated. Star–galaxy separation seems to be robust down to $i = 21$ mag. The solid line marks the boundary for selection of point sources (HLR $\leqslant$2.82).

All but seven of the 233 spectroscopically confirmed stars with $i < 21$ have HLR $\leqslant$ 2.82 pixels. Fitting a Gaussian function to the HLR distribution of these 233 stars, we find that the mean of the distribution is HLR = 2.23 pixel and $\sigma = 0.11$ pixel. Seven stars with $i < 21$ that have HLR measurements larger than 3 pixels have nearby sources that possibly affect the HLR measurements. There are four galaxies with $i < 21$ that have HLR $\leqslant$ 2.82 pixels, corresponding to a contamination rate of 1.7 per cent. Therefore, HLR $\leqslant$ 2.82 pixel seems to be a reliable selection criteria for point sources with $i < 21$. At fainter magnitudes, the separation between stars and galaxies seem to be more difficult since the galaxies start to become dominant. We find that between $i = 21$–22 mag, the contamination of the stellar sample by galaxies increases up to 28 per cent. The galaxy contamination rate for the entire sample between $i = 17$–22 is 10.1 per cent, consistent with the estimate of Schultheis et al. (2006) of 13.1 ± 2.3 per cent.

The HLR distribution for D2, D3 and D4 are similar to D1. Hence, we use the criteria $i < 21$ and HLR $\leqslant$ 2.82 to select point sources in all four fields.

4 WHITE DWARFS IN THE CFHTLS

4.1 White Dwarfs with $T_{\rm eff} > 7000$ K

Hot white dwarfs have blue colours and they are located in an otherwise relatively empty part of the colour–colour diagrams. Harris et al. (2003) found that white dwarfs can be identified from the SDSS photometry until the white dwarf sequence overlaps with the stellar locus at around $T_{\rm eff} = 7000$ K. However, hot subdwarfs and

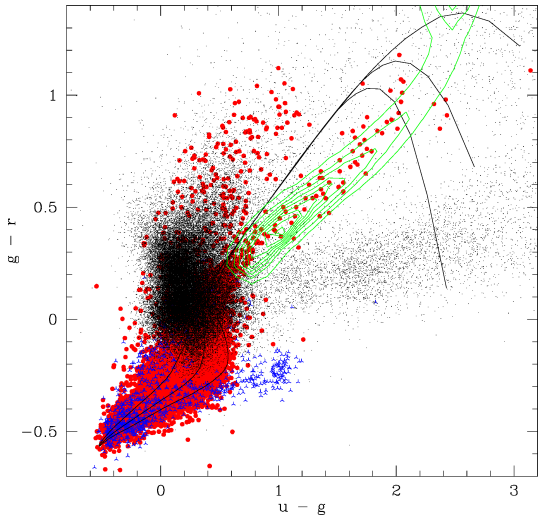

Figure 2. $(g-r)$ versus $(u-g)$ colour–colour diagram for the spectroscopically confirmed SDSS white dwarfs (red circles) and subdwarfs (blue points, Eisenstein et al. 2006; Kilic et al. 2006; Gates et al. 2004) and quasars (black points, Schneider et al. 2007). The solid lines show the colours of white dwarf model atmospheres of pure H for $\log g = 7$, 8 and 9 (from right- to left-hand side), respectively. The contours represent the stellar locus observed in the SDSS.

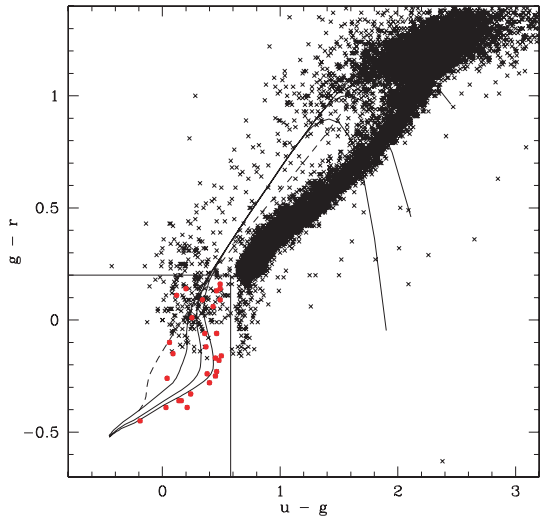

Figure 3. $(g-r)$ versus $(u-g)$ colour–colour diagram for the point sources selected from the D1, D2, D3 and D4 fields. The curves show the colours of white dwarf model atmospheres of pure H for $\log g = 7$, 8 and 9, respectively. The dashed line shows pure He WD models for $\log g = 8$. The dark solid lines show our selection region for hot WDs. Objects with *ugriz* colours that are consistent with WD models are shown as red circles.

especially quasars and faint blue galaxies may have similar colours to hot white dwarfs. Fan (1999) suggested that for a Galactic latitude of 60°, quasars outnumber white dwarfs for $g > 17$. Since the MEGACAM photometry data are obtained in the *ugriz* system, we can use the SDSS DR4 white dwarf catalogue and the DR5 quasar catalogue to assess the contamination of our white dwarf sample by quasars.

Fig. 2 presents $g-r$ versus $u-g$ colour–colour diagram for the spectroscopically identified white dwarfs (red circles, Eisenstein et al. 2006; Kilic et al. 2006; Gates et al. 2004), subdwarfs (blue points), and quasars (black points, Schneider et al. 2007). The contours show the stellar locus observed in the SDSS. The curves show the colours of white dwarf model atmospheres of pure hydrogen for $\log g = 7$, 8 and 9, respectively. This figure demonstrates that contamination from quasars can be significant, and should be taken into account. In order to limit the contamination by quasars, Eisenstein et al. (2006) used a colour cut of $g-r < 0.2$ to select their hot white dwarf candidates. They also used several other colour cuts to avoid halo subdwarfs.

Fig. 3 presents $g-r$ versus $u-g$ colour–colour diagram for the point sources in the CFHTLS D1, D2, D3 and D4 fields. Only objects with $17.00 \leqslant i \leqslant 21.00$ are displayed. The colours for pure H and pure He atmosphere white dwarfs in the MEGACAM photometry system (P. Bergeron, private communication) are shown as solid and dashed lines, respectively. The dark solid lines show our selection region for hot white dwarfs. The stellar sequence and the subdwarf sequence (at $u-g \sim 0.7$) are well populated. The overdensity of objects around $u-g = 0.3$ and $g-r = 0.2$ is likely to be caused by quasars.

We limit our selection region for white dwarfs to $u-g \leqslant 0.58$ in order to avoid subdwarfs, and to $g-r \leqslant 0.2$ in order to avoid quasars. There are 200 objects located in our selection region; a lot more than the expected number of white dwarfs in the CFHTLS Deep fields. This selection does not get rid off all the quasars. In order to eliminate the quasars from our sample, we compare the $u-g$, $g-r$, $r-i$ and $i-z$ colours of our candidates with the white dwarf model colours and the colours for the SDSS quasar sample. We divided the SDSS quasar sample into 0.1 redshift bins, averaged the colours for each bin, and compared the rms difference between the quasar colours, white dwarf model colours, and the colours for our selected objects. The use of all four colours eliminates the majority of the contaminating quasars from our sample as the quasars tend to have different colours compared to hot white dwarfs which tend to be blue in all colours. After this procedure, we are left with 30 candidate white dwarfs. We note that our procedure is not sensitive to white dwarfs with late-type star companions, and therefore we expect our catalogue to be incomplete.

We cross-identified these 30 candidate white dwarfs with the list of spectroscopically confirmed white dwarfs (McCook & Sion 2006) and the SDSS DR6 spectroscopy. Spectroscopy is available for 10 of our candidates; eight of them are white dwarfs, and two of them are quasars. Even the use of all four colours to identify white dwarfs did not eliminate all of the quasars in our sample. However, the majority of the objects in our final catalogue of 28 candidates should be bona fide white dwarfs. The coordinates, HLR, optical photometry, estimated effective temperatures and distances for our catalogue of 28 white dwarf candidates are given in Table 2.

4.2 Cool white dwarfs

The selection of cool white dwarfs using just optical photometry is not possible as they overlap with the stellar sequence (Kilic et al. 2004). However, collision-induced absorption (CIA) due to molecular hydrogen affects the optical colours of cool white dwarfs below 4000 K (Hansen 1998). Several of these ultracool white dwarfs have been found in the SDSS through follow-up spectroscopy of objects with i and z band deficits (Harris et al. 2001; Gates et al. 2004). These ultracool white dwarfs stand out in $r-i$ and $i-z$ colours.

Fig. 4 shows the $(r-i)$ versus $(g-r)$ diagram for the spectroscopically confirmed SDSS cool white dwarfs (Gates et al. 2004; Kilic et al. 2006) and quasars. The solid lines, contours and symbols are the same as in Fig. 2. The blue turn off of the white dwarf models

Table 2. White dwarf candidates in the CFHTLS Deep fields. Spectroscopically confirmed white dwarfs are marked with a ∗.

RA (J2000)	Dec. (J2000)	HLR(i) (pixels)	g (mag)	$u-g$ (mag)	$g-r$ (mag)	$r-i$ (mag)	$i-z$ (mag)	$T_{\rm eff}$ (K)	Distance (pc)
02:24:05.26	−04:22:16.3	2.55	18.23	0.46	−0.23	−0.21	−0.14	8228	134
02:24:23.76	−04:13:18.7	2.48	19.33	0.45	−0.17	−0.20	−0.15	7876	203
02:25:11.62	−04:56:10.5	2.44	17.75	0.46	−0.06	−0.10	−0.08	6725	72
02:25:12.69	−04:38:51.3	2.30	21.14	0.49	0.14	0.06	0.02	5487	213
02:25:58.18	−04:02:36.5	2.38	19.58	0.40	−0.28	−0.24	−0.14	9167	301
02:27:34.20	−04:22:28.6	2.63	20.41	0.12	0.11	−0.07	0.02	7255	249
02:27:46.37	−04:21:09.2	2.43	19.88	0.09	−0.15	−0.17	−0.12	9856	351
*09:58:43.49	+01:59:28.0	2.56	18.40	−0.19	−0.45	−0.37	−0.24	74 555	907
09:59:23.48	+02:31:43.5	2.54	19.16	0.04	−0.26	−0.24	−0.16	12 704	343
*09:59:36.96	+02:38:28.6	2.56	18.15	0.48	−0.18	−0.19	−0.13	7683	114
09:59:50.96	+02:24:30.7	2.66	20.99	0.34	0.09	−0.02	−0.05	6311	263
*10:00:05.66	+01:58:59.1	2.49	20.02	0.36	−0.06	−0.08	−0.09	7102	220
*10:00:49.67	+02:22:17.1	2.39	19.36	0.24	−0.33	−0.28	−0.18	11 493	369
14:17:07.56	+53:04:53.7	2.57	20.77	0.25	0.01	−0.10	−0.10	7375	319
14:17:24.11	+52:52:27.8	2.41	19.36	0.43	0.06	−0.02	−0.05	6131	121
14:17:27.11	+53:06:49.1	2.57	20.69	0.49	0.16	0.02	−0.04	5560	178
14:18:00.80	+52:24:39.7	2.68	19.44	0.37	−0.12	−0.13	−0.10	7600	194
*14:20:20.80	+52:15:49.6	2.37	16.88	0.03	−0.39	−0.33	−0.22	20 476	184
*14:21:18.20	+52:35:47.2	2.35	19.73	0.16	−0.36	−0.32	−0.22	14 117	515
*14:21:25.69	+53:04:54.6	2.42	19.12	0.46	0.13	0.03	−0.02	5680	90
*14:21:28.71	+52:13:18.2	2.44	19.04	0.38	−0.24	−0.25	−0.18	9167	232
22:13:26.37	−17:23:19.1	2.63	20.37	0.45	−0.25	−0.17	−0.27	8318	365
22:13:30.98	−18:01:44.5	2.75	20.99	0.49	0.09	0.02	−0.04	5736	222
22:14:05.73	−17:59:05.2	2.38	19.26	0.06	−0.10	−0.15	−0.12	9545	246
22:14:10.92	−17:40:36.6	2.55	19.89	0.14	−0.36	−0.26	−0.16	13 137	517
22:14:58.39	−18:07:42.6	2.44	20.38	0.50	−0.16	−0.13	−0.13	7173	280
22:15:15.23	−17:32:21.7	2.38	17.67	0.20	0.14	0.04	−0.02	6426	56
22:16:21.92	−17:44:08.0	2.32	20.30	0.21	−0.39	−0.25	−0.21	12 219	605

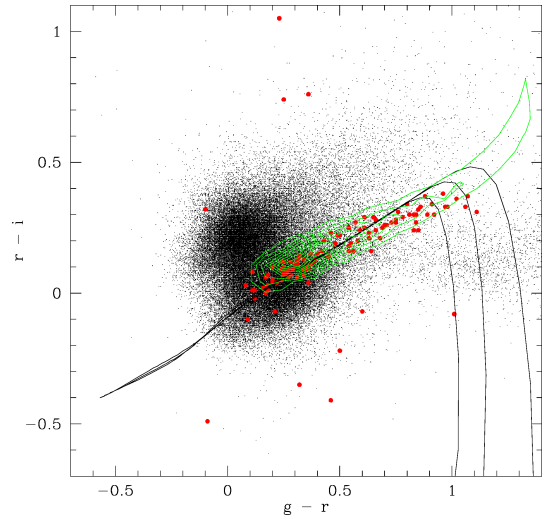

Figure 4. $(r-i)$ versus $(g-r)$ colour–colour diagram for the spectroscopically confirmed SDSS cool white dwarfs (red circles, Gates et al. 2004; Kilic et al. 2006) and quasars (black points, Schneider et al. 2007). The solid lines and contours are the same as in Fig. 2.

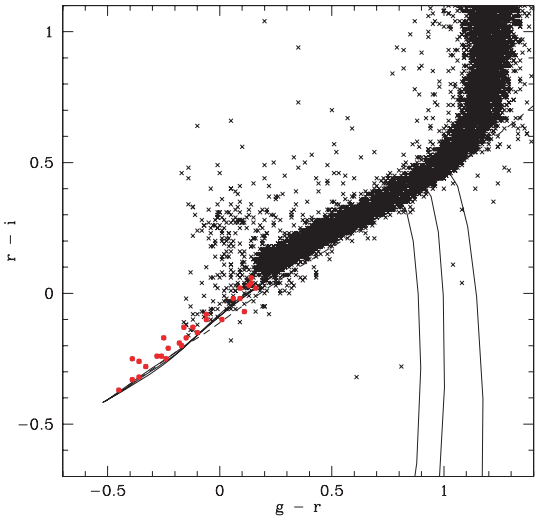

Figure 5. $(r-i)$ versus $(g-r)$ colour–colour diagram for the point sources selected from the D1, D2, D3 and D4 fields. The curves show the colours of white dwarf model atmospheres of pure H for $\log g = 7$, 8 and 9, respectively. The dashed line shows pure He WD models for $\log g = 8$. Objects with *ugriz* colours that are consistent with WD models are shown as red circles.

around $g-r \sim 1.1$ is due to the onset of CIA. The ultracool white dwarfs stand out in this diagram with blue $r-i$ colours compared to normal white dwarfs.

Fig. 5 presents the same colour–colour diagram for the CFHTLS Deep fields. The symbols are the same as in Fig. 3. There are several objects with $g-r$ and $r-i$ colours ($g-r > 0.5$ and $r-i < 0.2$) similar to the ultracool white dwarfs discovered in the SDSS. Instead of comparing their *ugriz* photometry to white dwarf model sequences, we compare them to the observed colours of ultracool

white dwarfs as the white dwarf model colours do not reproduce the observed sequence of ultracool white dwarfs. The SDSS ultracool white dwarfs have blue $i - z$ colours. We find that the $u - g$ and $i - z$ colours of the ultracool white dwarf candidates in the CFHTLS Deep fields are not consistent with being ultracool white dwarfs. Based on six ultracool white dwarfs discovered in 4330 deg^2 of SDSS spectroscopy data, Gates et al. (2004) estimated a density of 0.0014 deg^2 for $i < 20.2$ for ultracool white dwarfs. Hence, the non-detection of ultracool white dwarfs (for $i < 21$) in the CFHTLS Deep fields is not surprising.

5 DISCUSSION AND CONCLUSIONS

Using the third data release of the CFHTLS Deep fields, we have made an initial assessment of white dwarfs in these fields. Our main goal was to identify white dwarfs down to the limiting magnitude of the survey. However, we have discovered that star–galaxy separation is reliable down to $i = 21$ for the current data set. We have limited our point source selection to $i < 21$ and HLR $\leqslant 2.82$ pixels in order to minimize contamination by galaxies.

Our detailed analysis of the point sources in the CFHTLS Deep fields resulted in the discovery of 28 likely white dwarfs. Eight of these candidates are spectroscopically confirmed to be white dwarfs, which demonstrate that our selection process is efficient. The remaining 20 candidates require follow-up spectroscopy with an 8-m class telescope to be confirmed as white dwarfs.

We are not able to identify cool white dwarfs as they overlap with the stellar locus in various colour–colour diagrams. In addition, our photometric selection method does not include white dwarfs with late-type star companions. Even though we can identify ultracool white dwarfs using just photometry, we do not find any ultracool white dwarf candidates in these fields. The lack of ultracool white dwarfs in these fields is consistent with the small discovery rate of ultracool white dwarfs in the SDSS.

The total area covered by all four Deep fields is 3.6 deg^2. Did we find the majority of the white dwarfs in the CFHTLS Deep survey? The Besançon Galaxy model (Robin et al. 2003) predicts six thin disc, 0.2 thick disc and 0 halo white dwarfs per square degree for $i < 21$ (M. Schultheis, private communication). We have found a total of 28 white dwarf candidates; seven in D1, six in D2, eight in D3 and seven in D4. The Besançon Galaxy model slightly underestimates the number of white dwarfs in these fields. However, our white dwarf candidates probably include several quasars that were not recognized by our photometric selection algorithm. The two spectroscopically confirmed quasars and eight confirmed white dwarfs in our photometrically selected sample imply that contamination by quasars is of the order of 20 per cent in our final catalogue. Therefore, the number of white dwarfs in these fields may actually be around 22, consistent with the expected number of white dwarfs from the Besançon Galaxy model for 3.6 deg^2, 22 white dwarfs.

The CFHTLS Deep survey will include imaging of the same fields over 5 yr. Using a similar time-baseline for the SDSS Stripe 82, Vidrih et al. (2007) were able to obtain proper-motion measurement accuracy of $\sim$4.2 mas yr^{-1} down to $r = 21$ mag. Assuming that CFHTLS Deep survey will provide a comparable accuracy in proper-motion measurements, all but one of the white dwarfs in Table 1 would have 3σ proper-motion measurements if they have typical disc velocities of 40 km s^{-1}. Since the majority of white dwarfs in our sample have estimated distances within the thin disc population scale height, only a few are likely to be halo members. Proper-motion measurements for all of the halo white dwarfs would be detected at the 10σ level. At the end of the survey period, a complete catalogue of white dwarfs can be constructed through proper-motion selection.

ACKNOWLEDGMENTS

This material is based on observations obtained with MegaPrime/MegaCam, a joint project of CFHT and CEA/DAPNIA, at the CFHT which is operated by the National Research Council (NRC) of Canada, the Institut National des Science de l'Univers of the Centre National de la Recherche Scientifique (CNRS) of France and the University of Hawaii. This work is based in part on data products produced at TERAPIX and the Canadian Astronomy Data Centre as part of the CFHTLS, a collaborative project of NRC and CNRS. We thank P. Bergeron for providing his white dwarf models in MEGACAM photometric system. We gratefully acknowledge financial support of the Scientific and Technical Research Council of Turkey (TUBITAK, BIDEB-2221).

REFERENCES

Bertin E., Arnouts S., 1996, A&AS, 117, 393
Eisenstein D. J. et al., 2006, ApJS, 167, 40
Fan X., 1999, AJ, 117, 2528
Gates E. et al., 2004, ApJ, 612, L129
Gavazzi R., Soucail G., 2007, A&A, 462, 459
Hansen B. M. S., 1998, Nat, 394, 860
Harris H. C. et al., 2001, ApJ, 549, L109
Harris H. C. et al., 2003, AJ, 126, 1023
Harris H. C. et al., 2006, AJ, 131, 571
Kilic M., Winget D. E., von Hippel T., Claver C. F., 2004, AJ, 128, 1825
Kilic M. et al., 2006, AJ, 131, 582
Le Fevre O. et al., 2005, A&A, 439, 845
Liebert J., 1979, in van Horn H. M., Weidemann V., eds, IAU Colloq. 53, White Dwarfs and Variable Degenerate Stars, p. 146
Liebert J., Dahn C. C., Monet D. G., 1988, ApJ, 332, 891
McCook G. P., Sion E. M., 2006, VizieR Online Data Catalog, 3235
Munn J. A. et al., 2004, AJ, 127, 3034
Robin A. C., Reyle C., Derriere S., Picaud S., 2003, A&A, 409, 523
Schultheis M., Robin A. C., Reyle C., McCracken H. J., Bertin E., Mellier Y., Le Fevre O., 2006, A&A, 447, 185
Schneider D. P. et al., 2007, AJ, 134, 102
Szalay A. et al., 2003, ApJ, 591, 1
Vidrih S. et al., 2007, MNRAS, 382, 515
Winget D. E., Hansen C. J., Liebert J., Van Horn H. M., Fontaine G., Nather R. E., Kepler S. O., Lamb D. Q., 1987, ApJ, 315, L77

This paper has been typeset from a TEX/LATEX file prepared by the author.